UCSF

Title

Matched Analysis of Detailed Peripheral Blood and Tumor Immune Microenvironment Profiles in Bladder Cancer

Permalink

Journal

ISSN

Authors

Chen, Ji-Qing
Salas, Lucas A
Wiencke, John K
et al.

Publication Date
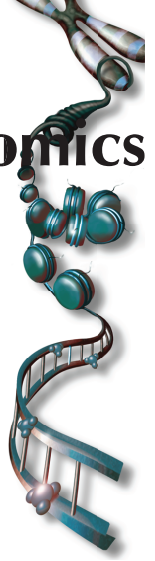
DOI

Matched analysis of detailed peripheral blood and tumor immune microenvironment profiles in bladder cancer

Ji-Qing Chen[1] (iD), Lucas A Salas[1] (iD), John K Wiencke[2] (iD), Devin C Koestler[3] (iD), Annette M Molinaro[2] (iD), Angeline S Andrew[4] (iD), John D Seigne[5] (iD), Margaret R Karagas[1] (iD), Karl T Kelsey[6] (iD) & Brock C Christensen*,[1,7] (iD)

[1]Department of Epidemiology, Geisel School of Medicine, Dartmouth College, Lebanon, NH 03766, USA
[2]Department of Neurological Surgery, University of California San Francisco, San Francisco, CA 94143, USA
[3]Department of Biostatistics & Data Science, University of Kansas Medical Center, Kansas City, KS 66160, USA
[4]Department of Neurology, Geisel School of Medicine, Dartmouth College, Lebanon, NH 03766, USA
[5]Department of Surgery, Section of Urology, Geisel School of Medicine, Dartmouth College, Lebanon, NH 03766, USA
[6]Departments of Epidemiology & Pathology & Laboratory Medicine, Brown University, Providence, RI 02912, USA
[7]Departments of Molecular and Systems Biology, Geisel School of Medicine, Dartmouth College, Lebanon, NH 03766, USA
*Author for correspondence: Tel.: +1 603 646 5411; Brock.Christensen@Dartmouth.edu

Background: Bladder cancer and therapy responses hinge on immune profiles in the tumor microenvironment (TME) and blood, yet studies linking tumor-infiltrating immune cells to peripheral immune profiles are limited. **Methods:** DNA methylation cytometry quantified TME and matched peripheral blood immune cell proportions. With tumor immune profile data as the input, subjects were grouped by immune infiltration status and consensus clustering. **Results:** Immune hot and cold groups had different immune compositions in the TME but not in circulating blood. Two clusters of patients identified with consensus clustering had different immune compositions not only in the TME but also in blood. **Conclusion:** Detailed immune profiling via methylation cytometry reveals the significance of understanding tumor and systemic immune relationships in cancer patients.

Plain language summary: Bladder cancer and treatment outcomes depend on the immune profiles in the tumor and blood. Our study, using DNA methylation cytometry, measured immune cell proportions in both areas. Patients were grouped based on immune status and consensus clustering. Results showed distinct immune compositions in the tumor, but not in blood, for hot and cold groups. Consensus clustering revealed two patient clusters with differing immune compositions in both tumor and blood. This detailed immune profiling highlights the importance of understanding the complex interplay between tumor and systemic immunity in bladder cancer patients.

Tweetable abstract: Bladder cancer immune profiles explored using DNA methylation cytometry. Tumor and blood immune compositions differ, highlighting the importance of detailed immune profiling. #BladderCancer #ImmuneProfiling

The immune system in the tumor microenvironment (TME) plays a critical role in bladder cancer development and treatment. Considerable evidence has indicated that bladder cancer cells are able to shape the microenvironment, resulting in immunosuppression beneficial for tumorigenesis. For example, due to the overexpression of S1PR1 in bladder cancer cells, TGF-β- and IL-10-induced Treg expansion has been shown to lead to suppression of cytotoxic T cells in the TME [1,2]. Numerous studies have indicated that myeloid-derived suppressor cells, which exhibit immunosuppressive properties, are recruited by bladder cancer cells with the secretion of CXCL2 and macrophage

migration inhibitory factor [3]. Infiltrating myeloid-derived suppressor cells are able to express arginase-1, inducible nitric oxide synthases and PD-L1 to induce Treg activation and suppress the function of T, B and natural killer (NK) cells [4–6]. Given that bladder cancer cells can escape from immune surveillance with the assistance of immunosuppressive cells, many treatments have been developed to target immunosuppressive cells and/or stimulate the activation of antitumor immune cells.

Following transurethral tumor resection, immunotherapies may be used in bladder cancer management. Instillation of Bacillus Calmette–Guérin (BCG) treatment is an immunotherapy used to prevent the recurrence and progression of non-muscle-invasive bladder cancer (NMIBC) [7]. Additionally, immune checkpoint inhibitors (ICIs) demonstrate significant efficacy in patients with BCG-refractory NMIBC, prevention of recurrence following cystectomy for muscle-invasive bladder cancer (MIBC) and in the management of metastatic disease [8]. BCG treatment uses the attenuated form of the tuberculosis vaccine, which induces an inflammatory reaction and activates antitumor immune cells, such as NK and CD8 T memory cells, within the TME [7,9]. ICIs are used to block the interaction of PD-1 with PD-L1, aiming to restore the activity of effector T cells against bladder cancer cells [8]. However, <30% of bladder cancer patients respond to immunotherapy [10–12]. One potential contribution to immunotherapy resistance is the immune landscape of the TME. For instance, patients with abundant T-cell infiltration in the TME, typically called immune hot, respond better to ICIs compared with patients with little immune cell infiltration, also known as immune cold tumors [13–16]. Currently, there is no standard definition of immune hot and cold tumors for bladder cancers, and a more complete understanding of the immune composition of the TME is required to improve treatments for bladder cancer.

Only a few studies have investigated both the tumor and peripheral blood immune status in bladder cancer. Existing work to date has been limited to tumor and peripheral blood neutrophil measures. For example, high neutrophil proportions in both peripheral blood and the TME have been associated with immunosuppressive effects in bladder cancer [17]. Additional works investigating other immune cell types within the bladder cancer microenvironment and their association with circulating immune profiles are needed to improve the management of bladder cancer.

Due to the critical role in gene regulation for cell lineage specification [18,19], DNA methylation profiles can be leveraged to estimate cell-type proportions [20–22]. The major advantages of DNA methylation cytometry are high accuracy and the ability to work in archival specimens [23–25]. Many studies have exploited DNA methylation cytometry in the cancer research field, including bladder cancer [25–28]. Currently, publicly available DNA methylation data for tumor tissue are predominantly from MIBCs, and thus information on NMIBCs is lacking as matched data from blood samples are uncommon. Here we obtained tumor tissues and matched blood samples from NMIBC and MIBC patients through a population-based case–control study [29–31]. We aimed to investigate the relationship of immune profiles in circulating peripheral blood with immune profiles in the TME in bladder cancer subtypes. As our samples were archival specimens, we performed DNA methylation cytometry to identify the immune profiles of both compartments. Recently, our group developed methods that enable the deconvolution of DNA methylation data quantifying cell types in the TME [32] and immune cell types in peripheral blood [20]. Here we identified and compared the distributions of immune landscapes in bladder cancer patient tumors and peripheral blood using DNA methylation.

Materials & methods
Study subjects & samples
The study subjects have been described in detail in prior research [29–31]. In brief, we included a subset of bladder cancer patients recruited in three phases from a population-based case–control study in New Hampshire [33]. For our research, we included 331 subjects diagnosed between July 1994 and June 1998 in the phase 1 study, 243 between July 1998 and December 2001 in the phase 2 study and 194 between July 2002 and December 2004 in the phase 3 study. Subjects from phases 1 and 2 were identified using the New Hampshire State Cancer Registry and hospital cancer registry, while subjects in phase 3 were only those included in the hospital cancer registry. Patients with both available blood and tumor samples (n = 88) were included in the present study. Among 88 subjects, the median time interval from the initial diagnosis to the blood draw was 207 days. All blood samples were stored at 4°C and then frozen within 24 h of blood draw. Overall 11% (n = 10) of patients received treatment with BCG, and blood samples were taken after treatment (median: 583 days). All tumor samples were primary tumors from the initial biopsy or surgical resection via transurethral resection of bladder tumor, which was generally taken around the time of initial diagnosis, and BCG was administered after transurethral resection.

Formalin-fixed, paraffin-embedded (FFPE) tumor specimens and pathology reports were requested from treating physicians/pathology laboratories with initial diagnoses. Bladder tumors were reviewed by a single pathologist and classified based on the WHO classification criteria [31]. DNA extraction was performed using the QIAamp DNA FFPE Tissue Kit (Qiagen, CA, USA). Study participants underwent an extensive in-person interview to gather comprehensive data on demographic characteristics and risk factors, including information on cigarette smoking history [29–31,33].

DNA extraction, qualification & bisulfite modification

Blood and tumor DNA extraction was performed using the Qiagen QIAamp DNA Blood Kit and QIAamp DNA FFPE Tissue Kit, respectively, according to the manufacturer's protocol. For FFPE DNA extraction, QIAamp DNA FFPE Tissue Kit (Qiagen 56404) and supplementary deparaffinization solution protocol (Qiagen 19093) were used. In brief, 20-μm sections were cut from the paraffin-embedded tissue and placed into 1.5-ml Eppendorf tubes. The paraffin was removed by adding 320 μl of deparaffinization solution, followed by vortexing and incubation at 56°C for 3 min. Next, 180 μl of Buffer ATL was added to the sample, vortexed and centrifuged for 1 min at 10,000 r.p.m., then 20 μl proteinase K was added to the lower, clear phase of the sample, mixed and incubated at 56°C for 1 h, followed by a second incubation at 90°C for 1 h. Samples were then centrifuged for 30 s at 10,000 rpm and the lower, clear phase was transferred into a new 2-ml microcentrifuge tube. Clear phase samples were then processed using the remaining steps of the standard QIAamp DNA FFPE Tissue Kit protocol.

We quantified and qualified the extracted DNA from tissue and blood using a Qubit™ 3.0 fluorometer (Life Technologies, CA, USA) and Fragment Analyzer (Advanced Analytical, IA, USA). Extracted DNA samples were conducted for bisulfite modification with EZ DNA Methylation Kit (Zymo Research, CA, USA) according to the instructions of the manufacturer. Approximately 50–250 ng of DNA was referred to Diagenode (NJ, USA) for EPIC array analysis.

DNA methylation profiling

Bisulfite-modified DNA samples were subjected to the Infinium™ MethylationEPIC BeadChip array (Illumina, Inc., CA, USA) and measured for their methylation intensity at >850,000 CpG sites. Probe intensity data (iDAT) files were processed via the *preprocessNoob* normalization method from the R package *minfi* [34]. *ENmix* [35], another R package, was performed for the quality control of probes. For sample selection, we set that samples with more than 5% of probes with a detection p-value $> 1.0 \times 10^{-6}$ would be excluded to distinguish from background noise; fortunately, all samples had good quality and were kept in the study. Probes were checked by observing any probes that were not missing in more than 10% of the samples. *BMIQ* [36] from the *watermelon* [37] R package was performed for probe-type normalization, and batch effects were corrected using *ComBat* [38]. Then, 119,258 probes previously described to be potentially cross-hybridizing, sex-specific, non-CpG methylation and SNP-associated were filtered [39]. In total, 746,980 were included in the final analysis (Figure 1A). The CpG loci were annotated with the *IlluminaHumanMethylationEPICanno.ilm10b4.hg19* [40] R package.

Statistical analysis

Cell-type proportions in the TME were inferred using hierarchical tumor immune microenvironment epigenetic deconvolution (HiTIMED; https://github.com/SalasLab/HiTIMED) [32], and circulating cell-type proportions of 12 cell types were estimated through the *projectCellType_CP* from the *FlowSorted.Blood.EPIC* R package [20]. The blood deconvolution method was applied to DNA methylation profiles of 12 immune cell types derived from peripheral blood. Employing the IDentifying Optimal Libraries algorithm, a deconvolution library tailored specifically to blood samples was generated. The 12 immune cell types in blood encompass neutrophils, eosinophils, basophils, monocytes, naive B cells, memory B cells, NK cells, naive CD4 T cells, memory CD4 T cells, naive CD8 T cells, memory CD8 T cells and Treg cells. The HiTIMED approach returns 17 cell types representative of three major TME components including the 12 immune cell types listed above plus dendritic cells, tumor, nontumor epithelial, endothelial and stromal cells. HiTIMED was developed involving the implementation of the *InfiniumPurify* pipeline and *limma* linear regression for library development, and it makes 20 sets of hierarchical libraries available for each of the 20 tumor types whose microenvironment cell types it can deconvolute. It is noteworthy that each deconvolution library uses distinct CpG loci, is intended for use in the specific biospecimen type and has been optimized for the respective sample types.
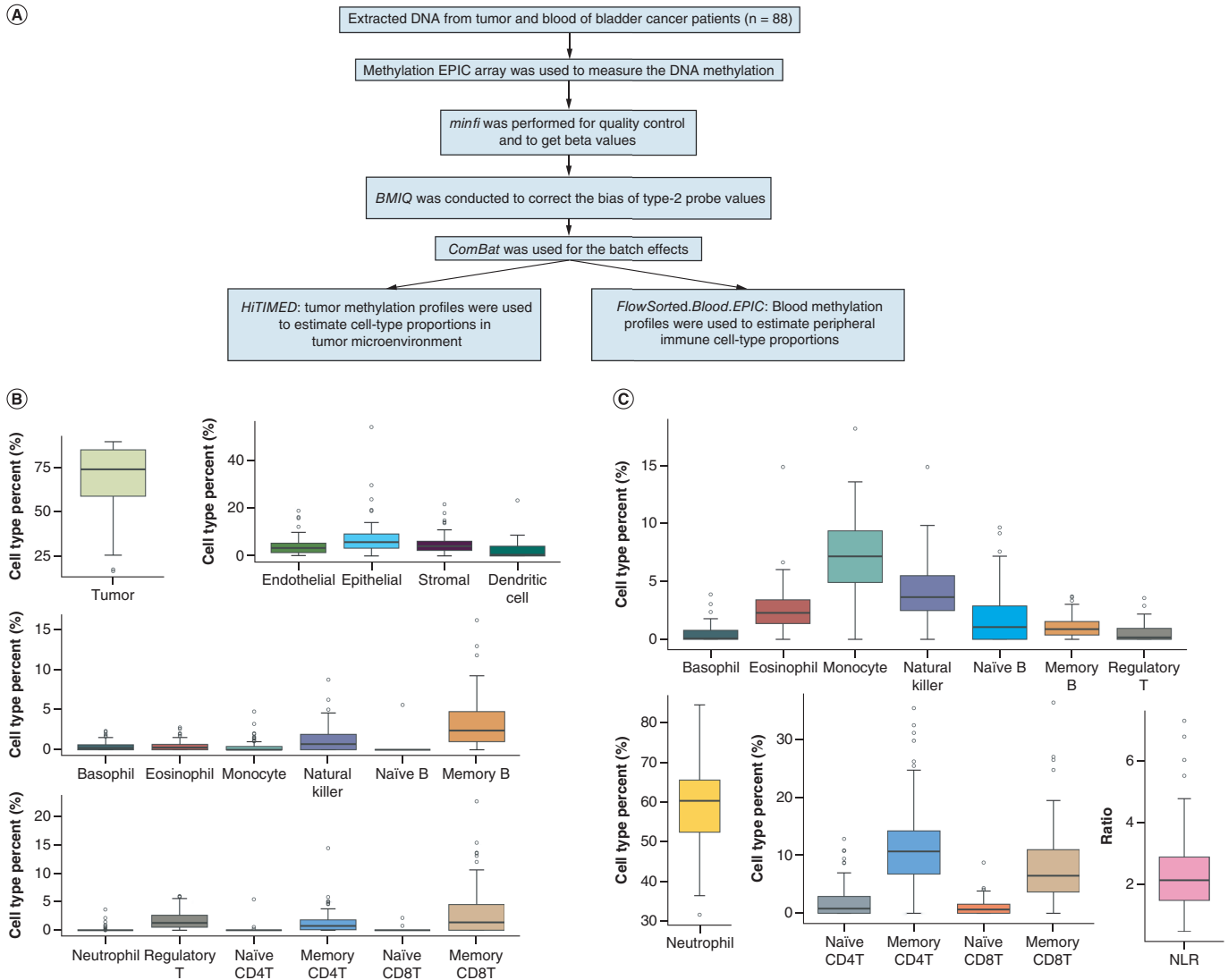
Figure 1. Data processing and cell distribution in tumor microenvironment and peripheral blood. (A) Data processing schematic. DNA was extracted from tumor tissues and matched blood samples of 88 bladder cancer patients. After serial preprocessing steps, DNA methylation profiles were applied to estimate cell-type proportions in **(B)** tumor tissues and **(C)** blood using *HiTIMED* and *FlowSorted.Blood.EPIC* methods respectively.
NLR: Neutrophil-to-lymphocyte ratio.

To integrate the information of cell-type proportions from tumor and blood, we grouped subjects using two methods. The first grouping method was according to the concept of immune hot and immune cold tumors. Because there is no standard definition of immune hot and immune cold tumors in bladder cancers, we grouped subjects based on the total percentage of antitumor immune cell-type proportions in the TME. If the sum of dendritic cell, NK and naive and memory subsets of CD4 T cell, CD8 T cell and B cell proportions was >5%, patients were assigned to the high immune infiltration (immune hot) group; otherwise they were assigned to the low immune infiltration (immune cold) group.

To also take an agnostic approach to grouping tumors by immune infiltration status, we performed consensus clustering [41] of standardized immune cell-type proportions in the TME as input using the *ConsensusClusterPlus* [42] R package with the setting of the following parameters and standardized immune cell-type proportions in the TME as input. The clustering algorithm was hierarchical clustering using a distance of 1 − Spearman correlation values. The number of repetitions of subsampling and clustering was 1000. To avoid overfitting, 80% of subjects were randomly selected for each repetition. The optimal number of clusters was determined by examining the cumulative

Table 1. Characteristics of the study subjects.			
	NMIBC (n = 75)	MIBC (n = 13)	All (n = 88)
Age			
Median (Q1, Q3)	67 (56, 71)	69 (64, 76)	67 (57, 72)
Sex			
Male	57 (76%)	8 (62%)	65 (74%)
Female	18 (24%)	5 (38%)	23 (26%)
Tumor grade			
Low	56 (75%)	3 (23%)	59 (67%)
High	19 (25%)	10 (77%)	29 (33%)
Tumor stage			
0a	61 (81%)	0 (0%)	61 (69%)
I	14 (19%)	0 (0%)	14 (16%)
II	0 (0%)	8 (62%)	8 (9%)
III	0 (0%)	2 (15%)	2 (2%)
IV	0 (0%)	3 (23%)	3 (4%)
Smoking status			
Never	12 (16%)	2 (15%)	14 (16%)
Former	40 (53%)	6 (46%)	46 (52%)
Current	21 (28%)	5 (39%)	26 (30%)
Missing	2 (3%)	0 (0%)	2 (2%)
BCG immunotherapy			
No	65 (87%)	13 (100%)	78 (89%)
Yes	10 (13%)	0 (0%)	10 (11%)
BCG: Bacillus Calmette–Guérin; NMIBC: Non-muscle-invasive bladder cancer; MIBC: Muscle-invasive bladder cancer.			

distribution function plot (Supplementary Figure 1), which guided our selection of two clusters. To test whether the immune composition in peripheral blood was different between groups, we performed permutational multivariate analysis of variance (PERMANOVA) using the *PERMANOVA* [43] R package, and the input was Aitchison distance matrix calculated by the *robCompositions* [44] R package. Differences in cell-type proportions between two groups generated via two methods (immune hot/cold and consensus clustering) were evaluated using the Wilcoxon rank sum test. Statistical comparisons between two categorical variables were performed using Fisher's exact test (two-tailed).

Results
Characteristics of subjects
The study group consisted of 75 NMIBC patients and 13 MIBC patients. The median age was 67 years; 65 (74%) were men; 59 (67%) had tumors in low grade; 46 (52%) and 26 (30%) were former and current smokers, respectively; and 10 (11%) patients received BCG treatment (Table 1). DNA methylation profiles obtained from the TME of 88 patients were used to estimate cell-type proportions in TME through HiTIMED, and the distribution of cell proportions is displayed in Figure 1B. The distribution of the matched methylation-derived immune cell profiles in the blood is shown in Figure 1C.

The potential influence of time elapsed between diagnosis and blood draw on the distribution of circulating immune cell-type proportions was considered. Thus, subjects were stratified according to the median time interval, allowing us to explore potential variations in immune profile distribution within peripheral blood across these groups. Our study findings revealed no discernible differences in circulating immune profiles between the stratified groups (Supplementary Figure 2). Furthermore, it is worth noting that BCG treatment could potentially impact the distribution of circulating immune cells. To assess this, we conducted a comparative analysis of immune cell-type proportions, both including and excluding patients who underwent BCG treatment. Our investigation revealed no significant differences in the distribution of circulating immune cells between groups including and excluding patients who received BCG treatment (Supplementary Figure 3).

Differences in tumor cell distribution between NMIBC & MIBC patients

We first investigated the association of tumor muscle-invasive status with the distribution of cell-type proportions in both the TME and peripheral blood. Within the TME, we observed that NMIBC patients had significantly lower memory B, NK, neutrophil, memory CD8 T, endothelial, stromal and dendritic cell proportions and a higher epithelial cell proportion compared with MIBC patients (Figure 2); however, no significant differences in circulating immune profiles were observed between NMIBC and MIBC patients (Supplementary Figure 4).

The impact of tumor immune infiltration on peripheral blood immune cell distribution

In recent years, several studies have reported that cellular immune composition within a tumor plays a critical role in tumor development and the response to immunotherapy, generating the concept of immune hot and cold tumors [13,14,45,46]. Because tumor-infiltrated immune cells translocate to tumor sites through the bloodstream, we assessed the association between immune cell-type proportions in TME and blood. Due to the lack of a standard definition of immune hot and cold tumors for bladder cancer, we clustered subjects based on the infiltrated antitumor immune cell proportions (the sum of dendritic cells, NK cells and naive and memory subsets of lymphocytes). Typically, the concept of immune hot and cold tumors is limited by diverse methods to assess the level of immune cell infiltration in tumors, and limited specificity of the immune cell types that are assessed. For instance, strong antitumor immune responses or abundant antitumor immune cell infiltration (e.g., with $CD3^+$ and $CD8^+$ cytotoxic T cells, NK cells) in the TME have been associated with better responses to immunotherapy [49]. Tumors with higher levels of infiltrating lymphocytes are often termed hot tumors, while those with lower levels are referred to as cold tumors [13,14,47–49]. The specific cutoff values may vary across studies and tumor types. Given that this was an exploratory analysis, we set the cutoff value for high and low immune infiltration tumors as 5%. The median value of infiltrated antitumor immune cell proportion is 7%. Antitumor immune cell proportion of <5% in the TME was defined as low immune infiltration (immune cold: n = 38), while tumors with infiltrating immune cell proportions >5% were in the high immune infiltration group (immune hot: n = 50). We found significant differences in the immune composition in the TME between the two groups (p = 0.001; PERMANOVA test). While our findings showed patients in the high immune infiltration group had higher eosinophil, memory CD4 T, memory CD8 T, NK, memory B and dendritic cell proportions in the TME compared with the low immune infiltration group, we did not observe any statistical differences in the immune composition in peripheral blood (p = 0.13; PERMANOVA test) or for individual cell types between the immune hot and immune cold patient groups (Figure 3). We conducted Fisher's exact test to determine whether there are associations between tumor infiltration and tumor characteristics. We observed that high antitumor immune infiltration was associated with tumor grade, stage and muscle invasiveness, but not with BCG treatment (Supplementary Table 1).

For NMIBC, patients were also stratified based on antitumor immune cell proportion (immune hot: n = 37; immune cold: n = 38). A significant distinction in immune composition within the TME emerged between immune hot and immune cold groups (p = 0.001; PERMANOVA test), while no significant differences were noted in the immune composition of peripheral blood (p = 0.16; PERMANOVA test). Similar to the overall cohort (NMIBC + MIBC), the immune hot NMIBC group exhibited higher proportions of eosinophils, memory CD4 T cells, memory CD8 T cells, NK cells, memory B cells and dendritic cells in the TME compared with the immune cold NMIBC group (Supplementary Figure 5). The Fisher's exact test results for NMIBC patients are presented in Supplementary Table 2.

Comparing tumor & blood immune cell distributions using consensus clustering

Next, we used an unbiased approach for grouping patients based on tumor immune infiltration with consensus clustering, resulting in two groups (group 1: n = 43; group 2: n = 45). We observed a significant difference in the immune composition in the TME between the two groups (p = 0.001; PERMANOVA test). Among nonimmune cell types, group 1 patients had higher endothelial and stromal cell proportions and a lower epithelial cell proportion in the TME compared with group 2 patients. Group 1 patients had significantly higher memory CD8 T, NK, memory B and dendritic cell proportions and lower basophil and monocyte proportions in the TME (Figure 4).

Unlike the more basic approach using antitumor immune cell percentage in the TME, with groupings from consensus clustering based on tumor immune cell proportions we observed statistical differences in the immune composition in peripheral blood (p = 0.01; PERMANOVA test). In addition, individual circulating immune profiles had significant differences between groups, including basophil, naive CD4 T and memory CD4 T cell types (Figure 4). Interestingly, some peripheral blood cell proportions with significant differences between groups
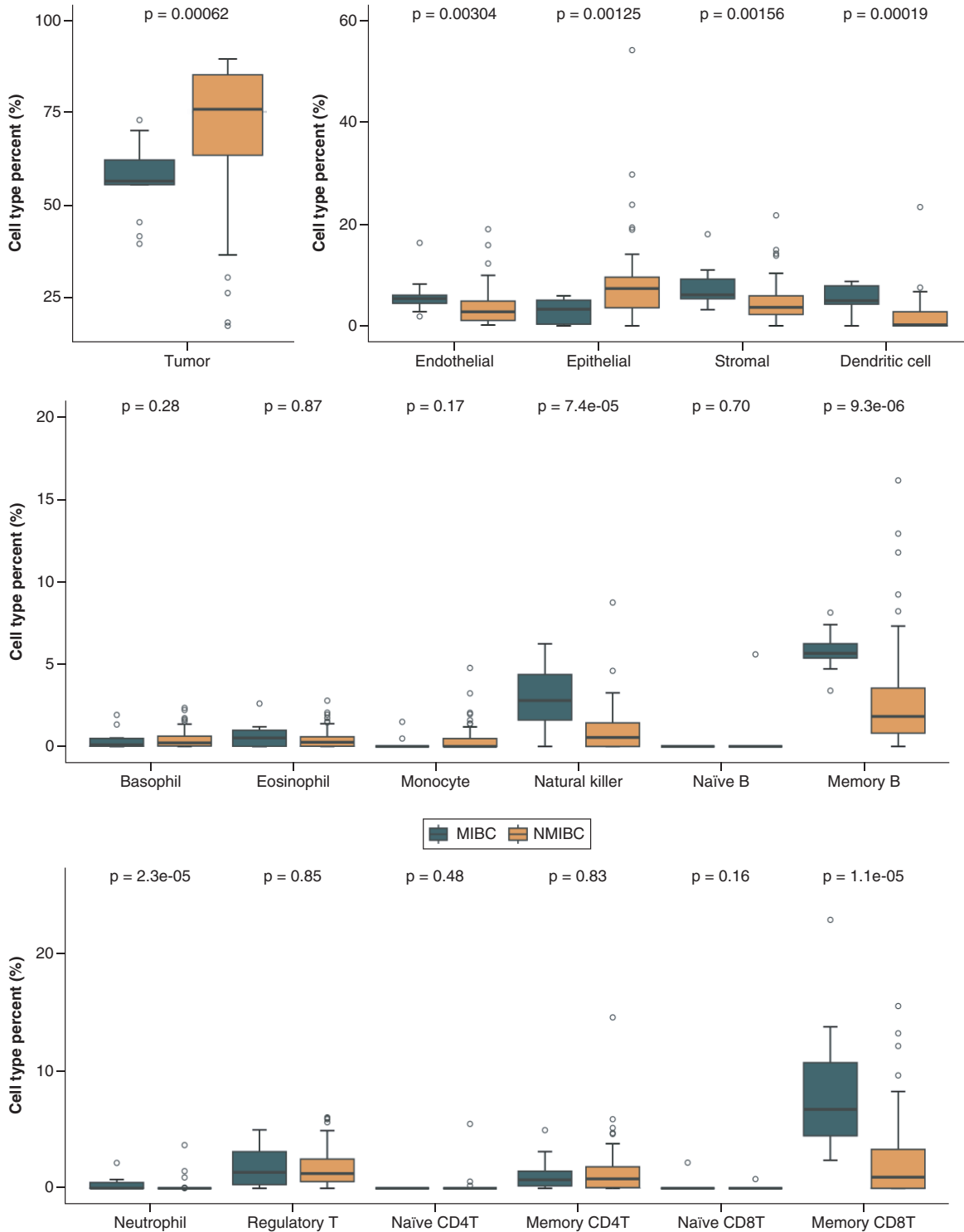
Figure 2. Cell profiles of tumor microenvironment in non-muscle-invasive and muscle-invasive bladder cancer patients. Differences in cell-type proportions between NMIBC and MIBC patients were evaluated using the Wilcoxon rank sum test.

MIBC: Muscle-invasive bladder cancer; NMIBC: Non-muscle-invasive bladder cancer.
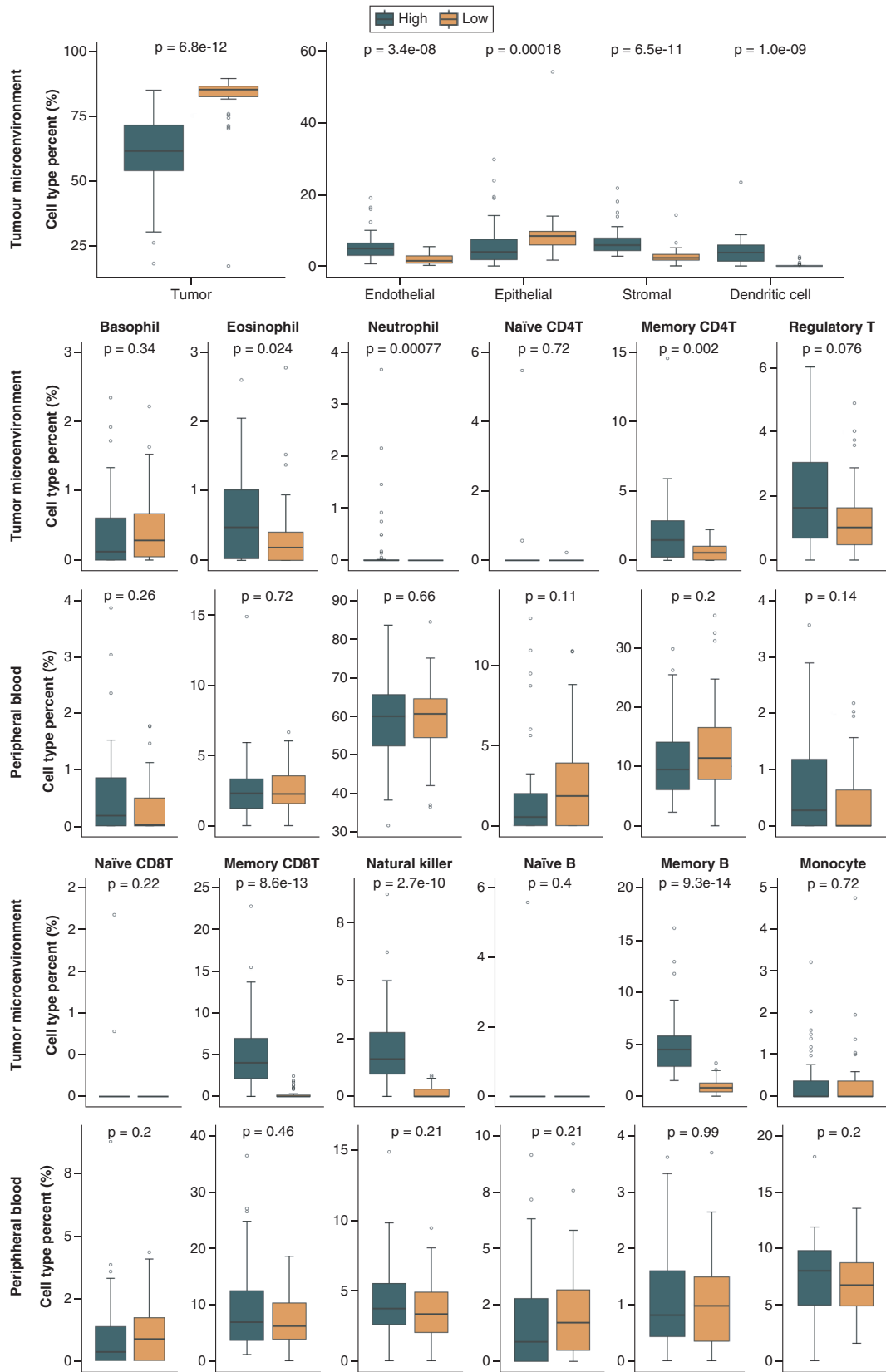
Figure 3.   Tumor and blood cell profiles distribution of two groups assigned by the proportion of antitumor immune infiltration. The high immune infiltration group (High) consisted of the 50 patients who had the sum of B, CD8 T, CD4 T, natural killer and dendritic cell proportions >5% in the tumor microenvironment. The low immune infiltration group (Low) consisted of the 38 patients who had the sum of B, CD8 T, CD4 T, natural killer and dendritic cell proportions ≤5% in the tumor microenvironment. Differences in cell-type proportions between two groups were evaluated using the Wilcoxon rank sum test.

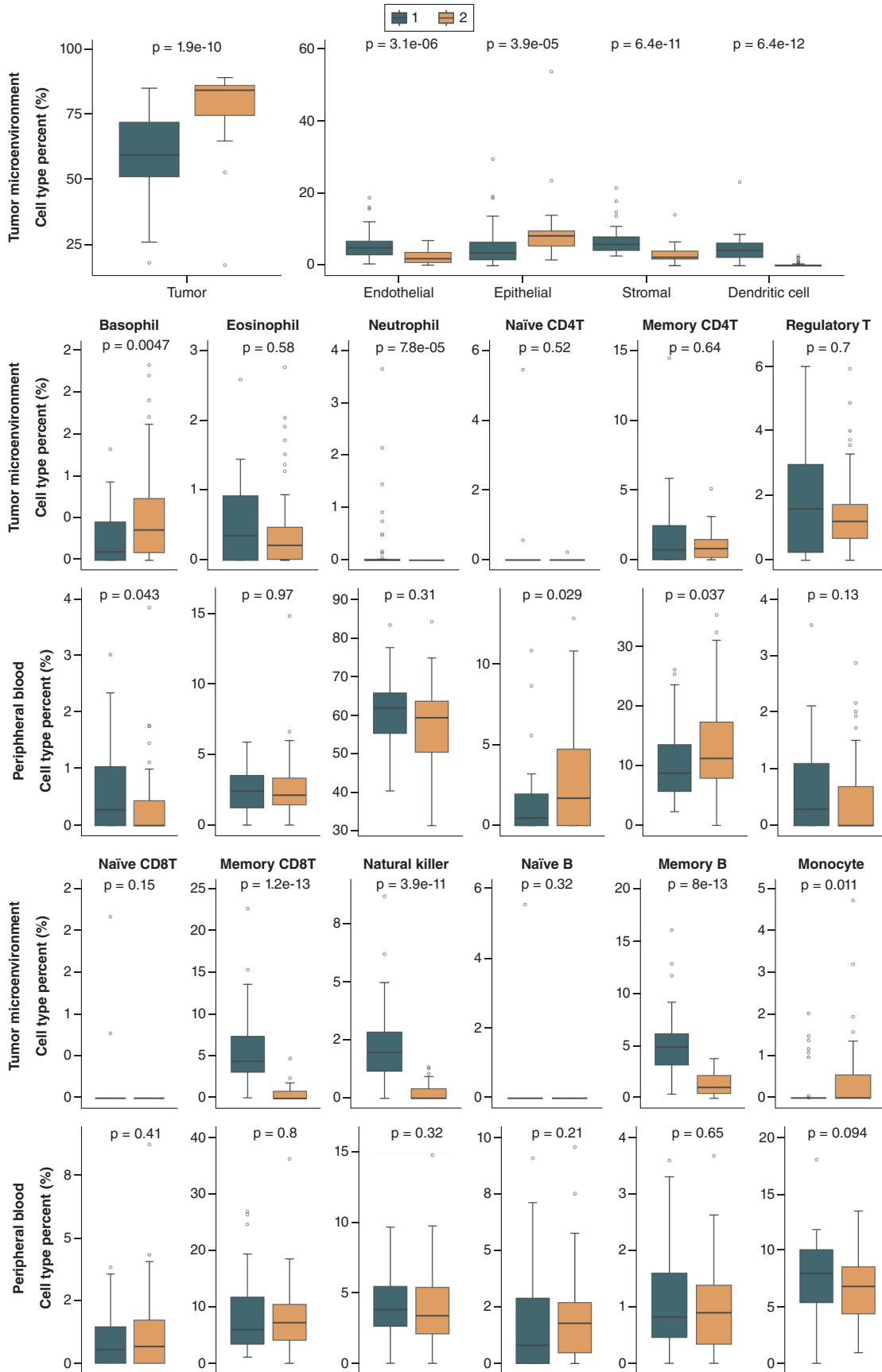**Figure 4.   Tumor and blood cell profiles distribution of two groups assigned by consensus clustering algorithm using tumor immune profiles as input.** Group 1 and group 2 consisted of 43 and 45 patients, respectively. Differences in cell-type proportions between two groups were evaluated using the Wilcoxon rank sum test.

Table 2. The distribution of subject characteristics within groups derived from consensus clustering.

	Group 1 (n = 43)	Group 2 (n = 45)	Fisher's exact test; two-tailed	
			Odds ratio (95% CI)	p-value
Tumor grade			14.24 (4.32–46.89)†	8.50E-7
Low	18 (42%)	41 (91%)		
High	25 (58%)	4 (9%)		
Tumor stage			17.68 (4.74–65.99)‡	4.46E-7
0a	19 (44%)	42 (94%)		
I–IV	24 (56%)	3 (6%)		
Muscle invasive			17.03 (2.1–137.9)§	0.0007
No	31 (72%)	44 (98%)		
Yes	12 (28%)	1 (2%)		
BCG treatment			4.91 (0.98–24.65)¶	0.047
No	35 (81%)	43 (96%)		
Yes	8 (19%)	2 (4%)		
Immune infiltration			82.0 (16.62–404.6)#	7.22E-14
Low	2 (5%)	36 (80%)		
High	41 (95%)	9 (20%)		

†Group 1 patients had 14.24-times the odds of having a high tumor grade compared with patients in group 2.
‡Group 1 patients exhibited 17.68-times the odds of having an invasive tumor stage (stage I–IV vs 0a) compared with patients in group 2.
§Group 1 patients had 17.03-times the odds of having muscle-invasive tumors compared with patients in group 2.
¶Group 1 patients had 4.91-times the odds of receiving BCG treatment compared with patients in group 2.
#Group 1 patients had 82-times the odds of having high antitumor immune infiltration compared with patients in group 2.
BCG: Bacillus Calmette–Guérin.

had the opposite direction of cell proportion differences observed in the tumor. For example, patients in group 1 had a lower basophil proportion in the TME but a higher basophil proportion in blood compared with group 2. Despite not reaching statistical significance, patients with a higher monocyte proportion in the TME (group 2) had a lower monocyte proportion in their blood (Figure 4). In addition, we found the grouping result was associated with tumor grade, stage, muscle-invasive status and BCG treatment (Table 2). Interestingly, the findings showed that group 1 patients demonstrated significantly increased odds of having an advanced tumor stage (stage I–IV vs 0a; odds ratio: 17.68; 95% CI: 4.74–66.00), having a high tumor grade (odds ratio: 14.24; 95% CI: 4.32–46.90), being MIBC patients (odds ratio: 17.03; 95% CI: 2.10–137.90) and having high antitumor immune infiltration (>5%; odds ratio: 82.0; 95% CI: 16.62–404.6) compared with patients in group 2 (Table 2).

The same methodology was applied to NMIBC patients exclusively (group 1: n = 27; group 2: n = 48). Once again, a significant difference in immune composition within the TME was observed between the two groups (p = 0.001; PERMANOVA test), with similar immune cell proportions compared with the overall cohort (NMIBC + MIBC) (Supplementary Figure 6). However, no statistical difference was found in the immune composition in peripheral blood between the two groups (p = 0.07; PERMANOVA test). Additionally, the grouping results were associated with tumor grade, stage, antitumor immune infiltration levels and BCG treatment (Supplementary Table 3). The tumor/node/metastasis stage for MIBC and NMIBC with the distributions for consensus clustering model results is shown in Supplementary Table 4.

Discussion

The objective of this study was to investigate the distribution of immune cells within the TME of bladder cancer and explore its potential association with circulating immune profiles. Initially, we employed the HiTIMED [32] approach to estimate the cell distribution in the TME. Our findings revealed a scarcity of naive lymphocytes (~0%) in tumor tissues, aligning with their rarity in nonlymphoid tissues except peripheral blood [50–53]. Furthermore, we utilized the *FlowSorted.Blood.EPIC* [20] method to infer immune profiles within matched blood samples. Unsurprisingly, the mean neutrophil-to-lymphocyte ratio (NLR), a prognostic marker in various cancer types, was found to be 2.3 (Q1–Q3: 1.5–2.9). This value slightly exceeded the normal range of 1–2, as NLR values above 2.3 in adults serve as an early indicator of pathological conditions and cancer development [54,55]. In past studies, peripheral blood NLR has been demonstrated to be associated with an increased risk of death and tumor recurrence in bladder cancer patients [28,56,57].

Taylor & Francis
Taylor & Francis Group

We conducted several comparisons using different clustering approaches to address a knowledge gap regarding the association of immune profiles in bladder cancer between two compartments. While no significant differences were observed in circulating immune profiles between patients with MIBC and NMIBC, higher proportions of NK cells, neutrophils, memory B cells, memory CD8 T cells and dendritic cells were found in the TME of MIBC compared with NMIBC patients. These findings were consistent with a previous study that reported significantly elevated CD3 and CD8 tumor-infiltrating lymphocyte cell counts in MIBC compared with NMIBC patients [58].

In order to investigate the association of immune distribution between two compartments, we initially adopted the concept of immune hot and cold tumors to categorize the groups, although no standardized definitions were available in previous studies. Significant variations in immune profiles within the TME were observed, indicating distinctive immune characteristics among the categorized groups. In contrast, no significant differences were detected in immune profiles within the peripheral blood between the groups, suggesting that the conventional classification of immune hot and cold tumors might be inadequate in capturing the intricate relationship of immune profiles between the two compartments.

Interestingly, when applying the consensus clustering approach to categorize subjects based on more detailed immune infiltration profiling data, significant differences in immune profiles emerged within the TME and in peripheral blood across the clustering groups. Of particular note, we observed an inverse relationship between basophil proportions in the TME and peripheral blood (Figure 4). Previous research exploring the association of basophils with bladder cancer demonstrated that high basophil counts in peripheral blood were linked to an increased hazard of recurrence in high-grade T1 bladder cancer patients undergoing BCG treatment [59]. In our study, patients with a high circulating basophil proportion (group 1) exhibited 17.68-times the odds of having an invasive tumor stage (stage I–IV vs 0a) compared with patients in group 2. Similarly, patients with a high circulating basophil proportion (group 1) had 14.24-times the odds of having a high tumor grade compared with patients in group 2. Our previous study also demonstrated that elevated basophil proportions in blood were associated with an increased risk of death in NMIBC patients, with patients exhibiting poor overall survival showing higher circulating basophil proportions [60]. Although no study is currently surveilling basophils in the TME of bladder cancer, tumor-infiltrating basophils in other cancer types have been reported to play a critical role in tumor progression [61–63]. In addition to basophils, group 1 patients exhibited significantly lower monocyte proportions in the TME but slightly higher monocyte and significantly lower CD4 T-cell proportions in peripheral blood. Numerous studies have indicated that a high monocyte-to-lymphocyte ratio in the blood is associated with poor bladder cancer outcomes [64–67]. Circulating monocytes can be recruited into the TME through tumor-derived chemokines [68], where they differentiate into tumor-associated macrophages, promoting tumor cell survival, local invasion and metastasis [69–71]. The lower monocyte proportion in the TME of group 1 patients may be attributed to the tumor's ability to facilitate the differentiation of infiltrating monocytes into tumor-associated macrophages. Further investigations are warranted to validate this inference. Our exploration aims to encourage a re-evaluation of existing paradigms, particularly conventional grouping methods like immune hot and cold, and stimulate further research avenues that incorporate more detailed approaches for immune profiling.

To explore potential bias arising from analyzing NMIBC and MIBC together, we conducted analogous analyses exclusively focusing on NMIBC patients. Essentially, in consensus clustering, the results remained similar regarding the direction of the immune profiles in the TME and peripheral blood, with only slight numerical variations (Figure 4 & Supplementary Figure 6). When evaluating how many patients were reclassified during consensus clustering by exclusively focusing on NMIBC patients, we found that only six patients (8%) were reclassified (Supplementary Table 5). This suggests that analyzing NMIBC and MIBC patients together does not impact the results in our case. However, it is important to note that our dataset has a limited sample size of MIBC patients, and further evaluation is needed if the sample size of MIBC increases.

Several potential limitations should be acknowledged in this study. Firstly, all blood samples were collected after diagnosis, with a median time interval of 207 days (Q1–Q3: 120–517). Although the elapsed time may impact the distribution of circulating immune profiles, we found that peripheral immune profiles exhibited similar distributions when stratified based on the median time interval. Secondly, BCG treatment has been shown to influence immune profiles in both the TME and the circulatory system [72–74]. Despite lacking the information for responsiveness and the number of treatment cycles for each patient with treatment (n = 10; 13%), we did a comparison for circulating immune distribution between the datasets, including patients with BCG treatment (n = 88) or not (n = 78), demonstrating similar distribution. Furthermore, the sample size ratio between NMIBC and MIBC is imbalanced. Future data collection efforts should focus on including more MIBC patients than

NMIBCs to address this issue. Also, because novel approaches to immune profiling are being applied and our sample size is limited, we underscore that this study is exploratory, hypothesis-generating. Additional investigations using methylation cytometry immune profiling in matched blood and tumor samples are needed in bladder cancer and other tumor types. However, publicly available datasets with DNA methylation data from tumor tissues and matched blood samples are currently lacking. Additionally, due to incomplete information, we were unable to investigate the influence of other confounders, such as alcohol consumption [75,76] and obesity [77,78], on immune cell distribution. Finally, further studies with larger and independent patient cohorts are needed to validate and confirm these preliminary results.

Conclusion

Taken together, these results suggest that further investigations are warranted to unravel the intricate interplay between local and systemic events in immune modulation against bladder cancer cells. Our study presents a potential opportunity facilitated by a detailed immune profiling approach that utilizes cell-specific methylation data to deconvolute the TME. This work has provided additional insights into data analysis encompassing both tumor and peripheral blood immune profiles. We believe our findings will provide valuable contributions to further understanding immunotherapy response and the underlying mechanisms of bladder cancer development. Our findings show that detailed immune profiles from methylation cytometry offer new approaches to discerning tumor and systemic immune status relationships in cancer patients.

Summary points

- Bladder cancer development and the response to therapy are influenced by immune profiles in the tumor microenvironment (TME) and peripheral blood.
- Despite the significance of immune involvement, studies investigating associations of tumor-infiltrating immune cell levels with circulating blood immune profiles are limited.
- We identified and compared the distributions of immune landscapes in bladder cancer patient tumors and peripheral blood using DNA methylation.
- Compared with non-muscle-invasive bladder cancer patients, muscle-invasive bladder cancer patients had higher dendritic cell, memory B, natural killer and memory CD8 T cell proportions in the TME.
- Patients with high antitumor immune infiltration had higher dendritic cell, eosinophil, memory CD4 T, memory CD8 T, natural killer and memory B cell proportions in the TME compared with the low antitumor immune infiltration group, but there were no differences in circulating immune profiles.
- With consensus clustering, patients in group 1 had significant differences in immune profiles in both TME and peripheral blood.
- Interestingly, group 1 patients had the inverse association of basophil proportions in blood and TME.
- This study not only clarifies the potential link between immune profiles in the two compartments but also underscores the promising opportunity to utilize the comprehensive immune profiling method based on methylation data.

Taylor & Francis
Taylor & Francis Group

References

Papers of special note have been highlighted as: ● of interest; ●● of considerable interest

1. Liu Y-N, Zhang H, Zhang L *et al.* Sphingosine 1 phosphate receptor-1 (S1P1) promotes tumor-associated regulatory T cell expansion: leading to poor survival in bladder cancer. *Cell Death Dis.* 10(2), 50 (2019).

2. Loskog A, Ninalga C, Paul-Wetterberg G, de la Torre M, Malmström P-U, Tötterman TH. Human bladder carcinoma is dominated by T-regulatory cells and Th1 inhibitory cytokines. *J. Urol.* 177(1), 353–358 (2007).

3. Zhang H, Ye Y-L, Li M-X *et al.* CXCL2/MIF-CXCR2 signaling promotes the recruitment of myeloid-derived suppressor cells and is correlated with prognosis in bladder cancer. *Oncogene* 36(15), 2095–2104 (2017).

4. Veglia F, Perego M, Gabrilovich D. Myeloid-derived suppressor cells coming of age. *Nat. Immunol.* 19(2), 108–119 (2018).

5. Wu K, Tan M-Y, Jiang J-T *et al.* Cisplatin inhibits the progression of bladder cancer by selectively depleting G-MDSCs: a novel chemoimmunomodulating strategy. *Clin. Immunol.* 193, 60–69 (2018).

6. Eruslanov E, Neuberger M, Daurkin I *et al.* Circulating and tumor-infiltrating myeloid cell subsets in patients with bladder cancer. *Int. J. Cancer* 130(5), 1109–1119 (2012).

7. Jiang S, Redelman-Sidi G. BCG in bladder cancer immunotherapy. *Cancers (Basel)* 14(13), 3073 (2022).

8. Lopez-Beltran A, Cimadamore A, Blanca A *et al.* Immune checkpoint inhibitors for the treatment of bladder cancer. *Cancers (Basel)* 13(1), 131 (2021).

9.   Sonoda T, Sugimura K, Ikemoto S-I, Kawashima H, Nakatani T. Significance of target cell infection and natural killer cells in the anti-tumor effects of bacillus Calmette-Guerin in murine bladder cancer. *Oncol. Rep.* 17(6), 1469–1474 (2007).

10. Davis JW, Sheth SI, Doviak MJ, Schellhammer PF. Superficial bladder carcinoma treated with bacillus Calmette-Guerin: progression-free and disease specific survival with minimum 10-year followup. *J. Urol.* 167(2 Pt 1), 494–500; discussion 501 (2002).

11. Suzman DL, Agrawal S, Ning Y-M *et al.* FDA Approval Summary: atezolizumab or pembrolizumab for the treatment of patients with advanced urothelial carcinoma ineligible for cisplatin-containing chemotherapy. *Oncologist* 24(4), 563–569 (2019).

12. Zhang T, Harrison MR, O'Donnell PH *et al.* A randomized phase 2 trial of pembrolizumab versus pembrolizumab and acalabrutinib in patients with platinum-resistant metastatic urothelial cancer. *Cancer* 126(20), 4485–4497 (2020).

13. Kather JN, Suarez-Carmona M, Charoentong P *et al.* Topography of cancer-associated immune cells in human solid tumors. *Elife* 7 doi: 10.7554/eLife.36967 (2018).

14. Peng M. Immune landscape of distinct subtypes in urothelial carcinoma based on immune gene profile. *Front. Immunol.* 13, 970885 (2022).

15. Yuen KC, Liu L-F, Gupta V *et al.* High systemic and tumor-associated IL-8 correlates with reduced clinical benefit of PD-L1 blockade. *Nat. Med.* 26(5), 693–698 (2020).

16. Eckstein M, Strissel P, Strick R *et al.* Cytotoxic T-cell-related gene expression signature predicts improved survival in muscle-invasive urothelial bladder cancer patients after radical cystectomy and adjuvant chemotherapy. *J. Immunother. Cancer* 8(1), e000162 (2020).

17. Shaul ME, Fridlender ZG. Cancer-related circulating and tumor-associated neutrophils – subtypes, sources and function. *FEBS J.* 285(23), 4316–4342 (2018).

18. Suelves M, Carrió E, Núñez-Álvarez Y, Peinado MA. DNA methylation dynamics in cellular commitment and differentiation. *Brief. Funct. Genomics* 15(6), 443–453 (2016).

19. Salas LA, Wiencke JK, Koestler DC, Zhang Z, Christensen BC, Kelsey KT. Tracing human stem cell lineage during development using DNA methylation. *Genome Res.* 28(9), 1285–1295 (2018).

20. Salas LA, Koestler DC, Butler RA *et al.* An optimized library for reference-based deconvolution of whole-blood biospecimens assayed using the Illumina HumanMethylationEPIC BeadArray. *Genome Biol.* 19(1), 64 (2018).

••   **Enhanced DNA methylation cytometry methodology to achieve high-resolution cell mixture deconvolution, enabling the discrimination of 12 distinct immune cell types in blood.**

21. Reinius LE, Acevedo N, Joerink M *et al.* Differential DNA methylation in purified human blood cells: implications for cell lineage and studies on disease susceptibility. *PLOS ONE* 7(7), e41361 (2012).

22. Houseman EA, Accomando WP, Koestler DC *et al.* DNA methylation arrays as surrogate measures of cell mixture distribution. *BMC Bioinformatics* 13(1), (2012).

••   **Developed methylation cytometry as a method for estimating immune profiles in peripheral blood.**

23. Titus AJ, Gallimore RM, Salas LA, Christensen BC. Cell-type deconvolution from DNA methylation: a review of recent applications. *Hum. Mol. Genet.* 26(R2), R216–R224 (2017).

24. Teschendorff AE, Zheng SC. Cell-type deconvolution in epigenome-wide association studies: a review and recommendations. *Epigenomics* 9(5), 757–768 (2017).

25. Wiencke JK, Koestler DC, Salas LA *et al.* Immunomethylomic approach to explore the blood neutrophil lymphocyte ratio (NLR) in glioma survival. *Clin. Epigenetics* 9(1), 1–11 (2017).

26. Wiencke JK, Molinaro AM, Warrier G *et al.* DNA methylation as a pharmacodynamic marker of glucocorticoid response and glioma survival. *Nat. Commun.* 13(1), 5505 (2022).

27. Muse ME, Carroll CD, Salas LA, Karagas MR, Christensen BC. Application of novel breast biospecimen cell-type adjustment identifies shared DNA methylation alterations in breast tissue and milk with breast cancer-risk factors. *Cancer Epidemiol. Biomarkers* 32(4), 550–560 (2023).

28. Chen JQ, Salas LA, Wiencke JK *et al.* Immune profiles and DNA methylation alterations related with non-muscle-invasive bladder cancer outcomes. *Clin. Epigenetics* 14(1), 1–14 (2022).

29. Baris D, Karagas MR, Verrill C *et al.* A case–control study of smoking and bladder cancer risk: emergent patterns over time. *J. Natl Cancer Inst.* 101(22), 1553–1561 (2009).

30. Kelsey KT, Hirao T, Schned A *et al.* A population-based study of immunohistochemical detection of p53 alteration in bladder cancer. *Br. J. Cancer* 90(8), 1572–1576 (2004).

31. Schned AR, Andrew AS, Marsit CJ, Zens MS, Kelsey KT, Karagas MR. Survival following the diagnosis of noninvasive bladder cancer: WHO/International Society of Urological Pathology versus WHO classification systems. *J. Urol.* 178(4), 1196–1200 (2007).

32. Zhang Z, Wiencke JK, Kelsey KT, Koestler DC, Christensen BC, Salas LA. HiTIMED: hierarchical tumor immune microenvironment epigenetic deconvolution for accurate cell type resolution in the tumor microenvironment using tumor-type-specific DNA methylation data. *J. Transl. Med.* 20(1), 1–17 (2022).

••   **Study that devised methylation cytometry for diverse cancer types to assess immune profiles in the tumor microenvironment.**

33. Karagas MR, Tosteson TD, Blum J, Morris JS, Baron JA, Klaue B. Design of an epidemiologic study of drinking water arsenic exposure and skin and bladder cancer risk in a US population. *Environ. Health Perspect.* 106(Suppl. 4), 1047–1050 (1998).

34. Aryee MJ, Jaffe AE, Corrada-Bravo H *et al.* Minfi: a flexible and comprehensive Bioconductor package for the analysis of Infinium DNA methylation microarrays. *Bioinformatics* 30(10), 1363–1369 (2014).

35. Xu Z, Niu L, Li L, Taylor JA. ENmix: a novel background correction method for Illumina HumanMethylation450 BeadChip. *Nucleic Acids Res.* 44(3), e20 (2016).

36. Teschendorff AE, Marabita F, Lechner M *et al.* A beta-mixture quantile normalization method for correcting probe design bias in Illumina Infinium 450 k DNA methylation data. *Bioinformatics* 29(2), 189–196 (2013).

37. Pidsley R, Y Wong CC, Volta M, Lunnon K, Mill J, Schalkwyk LC. A data-driven approach to preprocessing Illumina 450K methylation array data. *BMC Genomics* 14(1), 293 (2013).

38. Johnson WE, Li C, Rabinovic A. Adjusting batch effects in microarray expression data using empirical Bayes methods. *Biostatistics* 8(1), 118–127 (2007).

39. Zhou W, Laird PW, Shen H. Comprehensive characterization, annotation and innovative use of Infinium DNA methylation BeadChip probes. *Nucleic Acids Res.* 45(4), e22 (2017).

40. Hansen KD. IlluminaHumanMethylationEPICanno.ilm10b4.hg19: annotation for Illumina's EPIC methylation arrays (2017). https://bioconductor.org/packages/release/data/annotation/html/IlluminaHumanMethylationEPICanno.ilm10b4.hg19.html

41. Monti S, Tamayo P, Mesirov J, Golub T. Consensus clustering: a resampling-based method for class discovery and visualization of gene expression micoarray data. *Mach. Learn.* 52, 91–118 (2003).

42. Wilkerson MD, Hayes DN. ConsensusClusterPlus: a class discovery tool with confidence assessments and item tracking. *Bioinformatics* 26(12), 1572–1573 (2010).

43. Vicente-Gonzalez L, Vicente-Villardon JL. PERMANOVA: Multivariate Analysis of Variance Based on Distances and Permutations (2021). https://cran.r-project.org/web/packages/PERMANOVA/index.html
• **Introduces a method that is able to integrate the Aitchison distance matrix to assess statistical differences between two compositional datasets.**

44. Templ M, Hron K, Filzmoser P. robCompositions: an R-package for robust statistical analysis of compositional data. In: *Compositional Data Analysis: Theory and Applications.* Pawlowsky-Glahn V, Buccianti A (Eds). Wiley, 341–355 (2011).

45. Joyce JA, Fearon DT. T cell exclusion, immune privilege, and the tumor microenvironment. *Science* 348(6230), 74–80 (2015).

46. Lanitis E, Dangaj D, Irving M, Coukos G. Mechanisms regulating T-cell infiltration and activity in solid tumors. *Ann. Oncol.* 28(Suppl. 12), xii18–xii32 (2017).

47. Hegde PS, Karanikas V, Evers S. The where, the when, and the how of immune monitoring for cancer immunotherapies in the era of checkpoint inhibition. *Clin. Cancer Res.* 22(8), 1865–1874 (2016).

48. Wang L, Geng H, Liu Y *et al.* Hot and cold tumors: immunological features and the therapeutic strategies. *MedComm* 4(5), e343 (2023).

49. Galon J, Bruni D. Approaches to treat immune hot, altered and cold tumours with combination immunotherapies. *Nat. Rev. Drug Discov.* 18(3), 197–218 (2019).

50. Pillai S, Mattoo H, Cariappa A. B cells and autoimmunity. *Curr Opin. Immunol.* 23(6), 721–731 (2011).

51. Allman D, Pillai S. Peripheral B cell subsets. *Curr. Opin. Immunol.* 20(2), 149–157 (2008).

52. Sprent J. Circulating T and B lymphocytes of the mouse. I. Migratory properties. *Cell. Immunol.* 7(1), 10–39 (1973).

53. von Andrian UH, Mackay CR. T-cell function and migration. Two sides of the same coin. *N. Engl. J. Med.* 343(14), 1020–1034 (2000).

54. Wu L, Saxena S, Singh RK. Neutrophils in the tumor microenvironment. *Adv. Exp. Med. Biol.* 1224, 1–20 (2020).

55. Zahorec R. Neutrophil-to-lymphocyte ratio, past, present and future perspectives. *Bratisl. Lek. Listy* 122(7), 474–488 (2021).

56. Vartolomei MD, Porav-Hodade D, Ferro M *et al.* Prognostic role of pretreatment neutrophil-to-lymphocyte ratio (NLR) in patients with non–muscle-invasive bladder cancer (NMIBC): a systematic review and meta-analysis. *Urol. Oncol. Semin. Orig. Investig.* 36(9), 389–399 (2018).

57. Zhang Q, Lai Q, Wang S, Meng Q, Mo Z. Clinical value of postoperative neutrophil-to-lymphocyte ratio change as a detection marker of bladder cancer recurrence. *Cancer Manag. Res.* 13, 849–860 (2021).

58. Kerim I, Ammad A, Mahmood H, Al-zayadi FQJ. Comparative analysis of tumor infiltrating T Cells and serological markers between MIBC and NMIBC patients. *Medicolegal Updat.* 20(4), 770–775 (2020).

59. Ferro M, Di Lorenzo G, Vartolomei MD *et al.* Absolute basophil count is associated with time to recurrence in patients with high-grade T1 bladder cancer receiving bacillus Calmette–Guérin after transurethral resection of the bladder tumor. *World J. Urol.* 38(1), 143–150 (2020).

60. Chen J-Q, Salas LA, Wiencke JK *et al.* Genome-scale methylation analysis identifies immune profiles and age acceleration associations with bladder cancer outcomes. *Cancer Epidemiol. Biomarkers Prev.* 32(10), 1328–1337 (2023).

61. He X, Cao Y, Gu Y *et al.* Clinical outcomes and immune metrics in intratumoral basophil-enriched gastric cancer patients. *Ann. Surg. Oncol.* 28(11), 6439–6450 (2021).

62. Poto R, Gambardella AR, Marone G *et al.* Basophils from allergy to cancer. *Front. Immunol.* 13, 1056838 (2022).

63. Zhang J, Yin H, Chen Q *et al.* Basophils as a potential therapeutic target in cancer. *J. Zhejiang Univ. Sci. B* 22(12), 971–984 (2021).

64. Lin K-C, Jan H-C, Hu C-Y *et al.* Tumor necrosis with adjunction of preoperative monocyte-to-lymphocyte ratio as a new risk stratification marker can independently predict poor outcomes in upper tract urothelial carcinoma. *J. Clin. Med.* 10(13), 2983 (2021).

65. Zhu X, Wu S-Q, Xu R *et al.* The evaluation of monocyte lymphocyte ratio as a preoperative predictor in urothelial malignancies: a pooled analysis based on comparative studies. *Sci. Rep.* 9(1), 6280 (2019).

66. Liu J, Wu P, Lai S *et al.* Preoperative monocyte-to-lymphocyte ratio predicts for intravesical recurrence in patients with urothelial carcinoma of the upper urinary tract after radical nephroureterectomy without a history of bladder cancer. *Clin. Genitourin. Cancer* 19(3), e156–e165 (2021).

67. Shi H, Wang K, Yuan J *et al.* A high monocyte-to-lymphocyte ratio predicts poor prognosis in patients with radical cystectomy for bladder cancer. *Transl. Cancer Res.* 9(9), 5255–5267 (2020).

68. Chanmee T, Ontong P, Konno K, Itano N. Tumor-associated macrophages as major players in the tumor microenvironment. *Cancers (Basel)* 6(3), 1670–1690 (2014).

69. Pollard JW. Tumour-educated macrophages promote tumour progression and metastasis. *Nat. Rev. Cancer* 4(1), 71–8 (2004).

70. Zhang Q, Liu L, Gong C *et al.* Prognostic significance of tumor-associated macrophages in solid tumor: a meta-analysis of the literature. *PLOS ONE* 7(12), e50946 (2012).

71. Qian B-Z, Li J, Zhang H *et al.* CCL2 recruits inflammatory monocytes to facilitate breast-tumour metastasis. *Nature* 475(7355), 222–225 (2011).

72. Taniguchi K, Koga S, Nishikido M *et al.* Systemic immune response after intravesical instillation of bacille Calmette-Guérin (BCG) for superficial bladder cancer. *Clin. Exp. Immunol.* 115(1), 131–135 (1999).

73. Han J, Gu X, Li Y, Wu Q. Mechanisms of BCG in the treatment of bladder cancer – current understanding and the prospect. *Biomed. Pharmacother.* 129, 110393 (2020).

74. van Puffelen JH, Novakovic B, van Emst L *et al.* Intravesical BCG in patients with non-muscle invasive bladder cancer induces trained immunity and decreases respiratory infections. *J. Immunother. Cancer* 11(1), e005518 (2023).

75. Ratna A, Mandrekar P. Alcohol and cancer: mechanisms and therapies. *Biomolecules* 7(3), 61 (2017).

76. Laso FJ, Vaquero JM, Almeida J, Marcos M, Orfao A. Chronic alcohol consumption is associated with changes in the distribution, immunophenotype, and the inflammatory cytokine secretion profile of circulating dendritic cells. *Alcohol. Clin. Exp. Res.* 31(5), 846–854 (2007).

77. Dyck L, Prendeville H, Raverdeau M *et al.* Suppressive effects of the obese tumor microenvironment on CD8 T cell infiltration and effector function. *J. Exp. Med.* 219(3), e20210042 (2022).

78. Elisia I, Lam V, Cho B *et al.* Exploratory examination of inflammation state, immune response and blood cell composition in a human obese cohort to identify potential markers predicting cancer risk. *PLOS ONE* 15(2), 1–21 (2020).